

# DNA Binding Property and Antitumor Evaluation of Xanthone with Dimethylamine Side Chain

Rui Shen · Weihua Wang · Gengliang Yang

Received: 6 January 2014 / Accepted: 19 March 2014 / Published online: 6 April 2014  
© Springer Science+Business Media New York 2014

**Abstract** In this work, a xanthone derivative was obtained by cationic modification of the free hydroxyl group of xanthone with dimethylamine group of high pKa value. The interactions of xanthenes with DNA were investigated by spectroscopic methods, electrophoretic migration assay and polymerase chain reaction test. Results indicate that xanthenes can intercalate into the DNA base pairs by the hydrophobic plane and the xanthone with dimethylamine side chain may also bind the DNA phosphate framework by the basic amine alkyl chain, thus showing a better DNA binding ability than the xanthone. Furthermore, inhibition on tumor cells (ECA109, SGC7901, GLC-82) proliferation of xanthenes were evaluated by MTT method. Analysis results show that the xanthone with dimethylamine side chain exhibits more effective inhibition activity against three cancer cells than the xanthone. The effects on the inhibition of tumor cells *in vitro* agree with the studies of DNA binding. It means that the amine alkyl chain would play an important role in its antitumor activity and DNA binding property.

**Keywords** Xanthone · DNA binding mode · Antitumor evaluation

## Introduction

The targeting selectivity between small molecules and biological macromolecules may be attributed to the molecule recognition. Particularly, recognition of small molecules with DNA

on a molecular level becomes important for regulation of gene expression and study of drugs action *in vivo*. A better understanding of how to target DNA sites specifically will lead not only to novel chemotherapeutics but also to a greatly expanded ability for chemists to probe DNA and develop highly sensitive diagnostic agents [1–3]. The various compounds are being used at the forefront of many of these efforts. These compounds can non-covalently bind with DNA by intercalation for planar aromatic ring systems, groove binding for large or flexible molecules, and external electrostatic binding for cations. The decision about which mode to bind depends much on the sizes and configuration of the molecules [4–6]. So the stable, inert and water-soluble molecules containing spectroscopically active centers may be widely exploited for serving as probes of biological systems and showing excellent biological activities.

The numerous biological experiments have demonstrated that DNA is the primary intracellular target of anticancer drugs due to the interaction between small molecules and DNA. This interaction can cause DNA damage in cancer cells, inhibiting the division of cancer cells and resulting in cell death [7–10]. Therefore, the study of interactions between anticancer reagents and DNA are also very important to understand the mechanisms of their anticancer activities [11–15]. All the investigations are the basis of new and more efficient anticancer drugs design. We have been focusing on studying the DNA binding property of xanthenes. Xanthenes are symmetrical three-membered ring compounds with eight substitution positions which could bring a variety of interesting structures with diverse pharmacology activities [16–18]. The previous results indicate that the xanthenes could intercalate into the base pairs of DNA, lead to DNA damage, and inhibit cell proliferation finally. Furthermore, the different alkyl substitute groups in xanthenes would affect the DNA binding affinity and the biological activity significantly [19, 20].

R. Shen (✉) · W. Wang · G. Yang  
College of Pharmaceutical Sciences, Key Laboratory of  
Pharmaceutical Quality Control of Hebei Province, Hebei University,  
Baoding 071002, People's Republic of China  
e-mail: shenr05@126.com

Based on the above results, a xanthone with dimethylamine side chain was synthesized by incorporating cationic group with relatively high pKa value to improve the hydrophilicity of the hydrophobic xanthone scaffold and tune the affinity or mode of xanthone to DNA. Subsequently, we have investigated the DNA binding property of xanthenes and their effects on the growth of three human cancer cell lines, ECA109 (esophagus cancer), SGC7901 (stomach cancer) and GLC-82 (lung cancer) in vitro. The primary aims of these experiments are to gain some insight into the effect of structural factor in amine group substituted xanthone with DNA binding and offer an impetus for designing newer DNA directed therapeutic agents.

## Experimental

### Materials

Xanthenes were prepared according to the literatures with some improvements [18, 21]. Calf thymus DNA (ct DNA) and ethidium bromide (EB) were purchased from Sigma-Aldrich Co. LLC. The pUC18 plasmid DNA was purchased from Takara Biotechnology (Dalian) Co. Ltd. The primers were purchased from Sangon Biotech (Shanghai) Co. Ltd. The Taq DNA polymerase was purchased from New England Biolabs (Beijing) Ltd. Other chemicals were reagent grade without further purification.

### Measurements

Electrospray ionization mass spectra (ESI-MS) were performed on a Bruker apex ultra 7.0 T Fourier transform mass spectrometer and <sup>1</sup>H NMR spectra were recorded by using a Bruker AVANCE III 600 spectrometer. The UV–Vis absorption spectra were recorded by using a Varian Cary 100 spectrophotometer, the fluorescence emission spectra were recorded by using a Hitachi F-4600 spectrofluorimeter, and the circular dichroic (CD) spectra were recorded by using a Bio-Logic MOS-450 spectrometer, respectively. The polymerase chain reaction (PCR) was performed on a PE 9700 thermal cycler. The electrophoresis bands of DNA were imaged by using a Tanon-1600 gel imager under UV light. The absorbance of MTT assay was recorded on a Bio-Tek Microplate Reader.

The measurements involving in the interaction of xanthenes with ct DNA were carried out in Tris–HCl buffer

(5 mM Tris, 50 mM NaCl and adjusted to pH 7.4 with HCl). The solution of ct DNA purity ( $A_{260}: A_{280} > 1.80$ ) and concentration ( $\epsilon = 6,600 \text{ M}^{-1} \text{ cm}^{-1}$  at 260 nm) was checked by UV–Vis spectrometer [22, 23]. The electrophoretic migration assay of plasmid DNA was carried out in Tris–HCl buffer (pH 7.4). PCR amplification was carried out in Themopol buffer (20 mM Tris–HCl, 10 mM KCl, 10 mM  $(\text{NH}_4)_2\text{SO}_4$ , 2 mM  $\text{MgSO}_4$ , 0.1 % Triton X-100, pH 8.8). Xanthenes were first dissolved in a minimum amount of DMSO (0.5 % of the final volume) and then diluted with the corresponding buffer to the required concentrations.

### Preparation of Xanthenes 1–2

The synthetic route of xanthone (1) and its dimethylamine side chain substituent (2) is shown in Fig. 1. Compound 1 was synthesized from the condensation of  $\gamma$ -resorcylic acid with resorcinol in the presence of anhydrous zinc chloride and phosphorus oxychloride as a condensing agent. Aminelation of 1 with amine alkyl halides in acetone afforded 2 in good yields. All the crude products were purified by chromatography on a silicagel column and recrystallized to afford 1–2 as yellow solids.

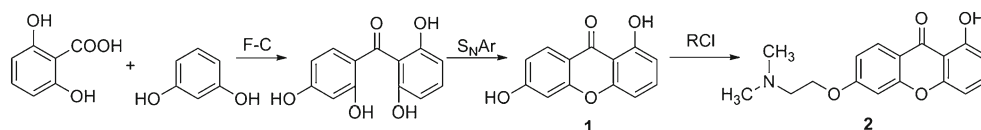
**1, 6-dihydroxy-9H-xanthen-9-one (1)** Yield 36.5 %, ESI-MS:  $m/z$  229.1  $[\text{M}+\text{H}]^+$ , <sup>1</sup>H NMR (600 MHz, DMSO-d<sub>6</sub>):  $\delta$  12.86 (s, 1 H), 11.22 (s, 1 H), 8.06–8.03 (d, 1 H), 7.71–7.65 (t, 1 H), 7.04–7.02 (d, 1 H), 6.97–6.94 (t, 1 H), 6.93–6.88 (t, 1 H), 6.80–6.78 (d, 1 H) ppm.

**6-(2-(dimethylamino)ethoxy)-1-hydroxy-9H-xanthen-9-one (2)** Yield 85.6 %, ESI-MS:  $m/z$  300.1  $[\text{M}+\text{H}]^+$ , <sup>1</sup>H NMR (600 MHz, CDCl<sub>3</sub>):  $\delta$  12.79 (s, 1 H), 8.16–8.18 (d, 1 H), 7.54–7.57 (t, 1 H), 6.98–6.99 (dd, 1 H), 6.88–6.90 (m, 2 H), 6.78–6.79 (d, 1 H), 4.20–4.22 (t, 2 H), 2.84 (s, 2 H), 2.40 (s, 6 H) ppm.

### DNA Interactions

Absorption and fluorescence titration experiments were performed by fixing the xanthenes concentration as constant at 5 and 10  $\mu\text{M}$ , respectively, while varying the concentration of ct DNA. The competitive binding experiment was carried out by maintaining the EB and ct DNA concentration at 2 and 30  $\mu\text{M}$ , respectively, while increasing the concentration of xanthenes. Fitting was completed by using an Origin 7.5

**Fig. 1** Synthetic route for xanthenes 1–2



spreadsheet, where values of the binding constants  $K_b$  and quenching constant  $K_q$  were calculated.

The CD spectra of DNA were scanned in the range of 200–400 nm by increasing compound/DNA ratio ( $r=0, 1/3$ ) at 25.0 °C. The optical chamber of the CD spectrometer was deoxygenated with dry nitrogen before use and kept in a nitrogen atmosphere during experiments. Scans were accumulated and automatically averaged. The spectra represented the average of three scans without the buffer background.

In the electrophoretic migration assays, xanthenes and 0.25  $\mu\text{g}$  pUC18 plasmid DNA were mixed and brought to 25  $\mu\text{L}$  by Tris–HCl buffer. All samples were incubated at 25 °C in the dark for 4 h. Then the DNA migration rate was detected by 1.0 % agarose gel electrophoresis in TBE (Tris-borate-EDTA) buffer (pH 8.0). The tests were repeated triplicate.

PCR amplifications were performed in a 25  $\mu\text{L}$  reaction mixture containing 0.1  $\mu\text{g}$  plasmid pEGFP-N1 DNA, 0.4  $\mu\text{M}$  of each primer (5'TCAGGTTTCAGGGGAGGTGTG3' (forward) and 5'AAGGCTACGTCCAGGAGCGCA3' (reverse)), 0.2 mM of each dNTP (deoxy-ribonucleoside triphosphate), 2.5  $\mu\text{L}$  of 10 $\times$ Themopol buffer and 1.5 U DNA Taq polymerase. The parameters were as follows: after heating at 95 °C for 5 min, 30 cycles were carried out including 50 s at 94 °C, 50 s at 55 °C, and 30 s at 72 °C. A final 5 min elongation was performed at 72 °C. The final product was analyzed on 1.5 % agarose gel electrophoresis in TBE buffer. In the experimental group, xanthenes and forward primer or reverse primer were premixed, incubated at 4 °C for 6 h, and then used for the PCR to study the effect on single stranded DNA. In the control group, xanthenes were added into the reaction mixtures directly for the PCR to detect the effect on Taq DNA polymerase. The experiments were repeated triplicate.

## In Vitro Antitumor Potency

The cells were plated in 96-well culture plates at density of 50,000 cells per well and incubated for 24 h at 37 °C in a water-atmosphere (5 %  $\text{CO}_2$ ). The xanthenes were dissolved in DMSO and diluted with culture medium (DMSO final concentration <0.5 %) to the required concentrations prior to use. After addition, the different concentration of xanthenes (10  $\mu\text{L}$ /well) were incubated with the cells for 68 h, 10  $\mu\text{L}$  of aqueous MTT solution (5 mg/mL) was added to each well, and the cells were incubated continually for another 4 h. The medium was removed and DMSO (100  $\mu\text{L}$ /well) was added. Subsequently, absorbance was recorded at 570 nm. All experiments were performed in triplicate and each experiment was repeated at least three times.

## Results and Discussion

### Electronic Absorption Spectra

The electronic absorption spectroscopy is one of the most useful techniques for DNA-binding studies of small molecules. As shown in Fig. 2, in the absence of DNA, the UV–Vis spectra of **1** has a strong  $\pi$ – $\pi^*$  transitions band at  $\lambda_{\text{max}}=230$  nm, a weak  $\pi$ – $\pi^*$  transitions band at  $\lambda_{\text{max}}=302$  nm and a medium  $n$ – $\pi^*$  transitions band at  $\lambda_{\text{max}}=358$  nm, while **2** has a strong  $\pi$ – $\pi^*$  transitions band at  $\lambda_{\text{max}}=230$  nm, a medium  $\pi$ – $\pi^*$  transition at  $\lambda_{\text{max}}=302$  nm and a weak  $n$ – $\pi^*$  transitions band at  $\lambda_{\text{max}}=358$  nm. With increasing DNA concentration, the absorption bands of the two compounds exhibit visible hypochromism as well as slight bathochromism. These variations are indicative of the intercalation mode between the

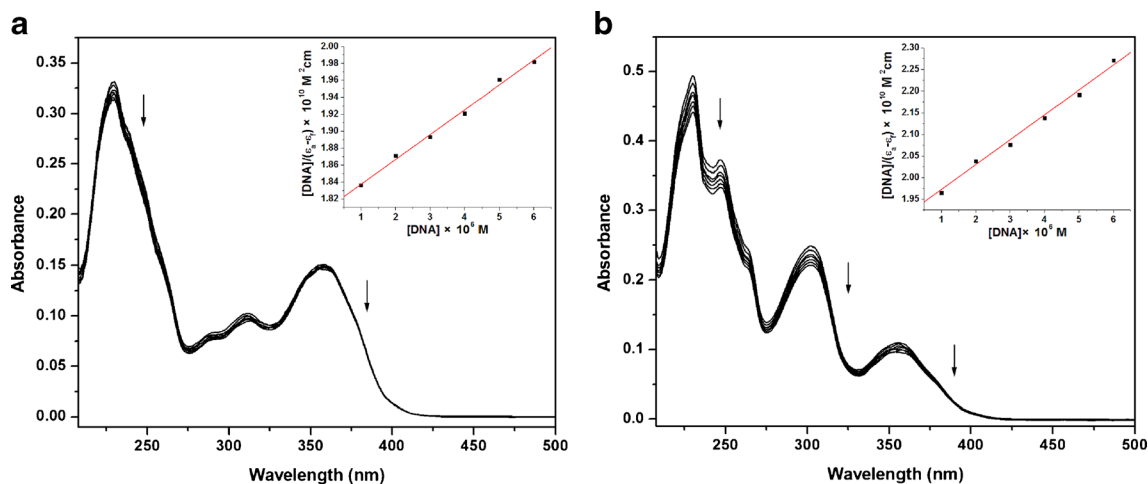


**Fig. 2** UV–Vis absorption spectra of **1** (a) and **2** (b) upon addition of ct DNA.  $C_{\text{xanthenes}}=5 \mu\text{M}$ ,  $C_{\text{DNA}}=0, 1, 2, 3, 4, 5, 6 \mu\text{M}$ . The arrow indicates the absorbance decreases upon increasing DNA concentration. The inset is plot of  $[\text{DNA}]/(\epsilon_b - \epsilon_f)$  versus  $C_{\text{DNA}}$  for the titration of DNA to xanthenes

compounds and ct DNA, involving a strong  $\pi$ -stacking interaction between the compounds and DNA base pairs [24, 25].

From the absorption data, the binding constant  $K_b$  is determined by using the Eq. (1),

$$[\text{DNA}] / (\varepsilon_a - \varepsilon_f) = [\text{DNA}] / (\varepsilon_b - \varepsilon_f) + 1 / K_b (\varepsilon_b - \varepsilon_f), \quad (1)$$

where [DNA] is the concentration of ct DNA in base pairs,  $\varepsilon_a$ ,  $\varepsilon_f$  and  $\varepsilon_b$  are the apparent extinction coefficient correspond to  $A_{\text{obsd}}/[\text{M}]$ , the extinction coefficient for the free compound and the extinction coefficient for the compound in the fully bound form, respectively [26]. In plots of  $[\text{DNA}] / (\varepsilon_a - \varepsilon_f)$  versus [DNA],  $K_b$  is given by the ratio of slope to the intercept (Fig. 2a–b, inset). The binding constant  $K_b$  for **1** and **2** are  $(1.58 \pm 0.12) \times 10^4 \text{ M}^{-1}$  and  $(3.26 \pm 0.19) \times 10^4 \text{ M}^{-1}$ , respectively. This means that **2** exhibits stronger binding affinity towards DNA.

### Fluorescence Spectra

Concomitant with the hypochromism in the absorption spectra of xanthenes upon addition of ct DNA, an obvious fluorescent emission enhancement of **1** at 450 nm occurs (Fig. 3a.). The result suggests that **1** can be protected efficiently from collision of water molecules by the hydrophobic environment inside the DNA helix. It indicates that **1** can insert between DNA base pairs deeply, which is similar to other intercalators and is consistent with the above absorption spectra results [27]. However, the fluorescence intensity of **2** decreases steadily upon increasing ct DNA concentration at 450 nm (Fig. 3b.). This phenomenon may be attributed to the quenching by the high negative charge of DNA. Because the phosphate groups of DNA with a negatively charged may

form a polyanion. And the amine moiety with high pKa values is more likely to be protonated and develop a cationic charge, which is quenched by the high negative charge of DNA easily.

From the fluorescence change (Fig. 3a–b, inset), **1** follows nearly linear variation and **2** follows a downward sloping curve. These indicate only one binding process in **1** to DNA, and more than one binding process in **2** to DNA. It may be concluded that **1** binds to DNA solely by intercalation mode and **2** binds to DNA not only by intercalation mode but also would be attracted to the electronegative phosphate framework, forming a surface bonding mode.

### Competitive Binding Experiment

As further proof, the DNA-EB adduct fluorescence quenching method can be used to determine the binding mode and affinity of the compound to DNA [28]. Figure 4 shows the emission spectra of DNA-EB system upon the increasing amounts of xanthenes. The emission intensity of DNA-EB system at 605 nm decreases upon increasing the concentration of xanthenes, which due to the translocation of EB from a hydrophobic environment to an aqueous environment [29]. It indicates that xanthenes could displace EB from the DNA-EB system. Such a characteristic change is often observed in intercalative DNA interactions [30].

According to the classical Stern-Volmer Eq. (2),

$$F_0 / F = 1 + K_q [Q], \quad (2)$$

where  $F_0$  and  $F$  represent the emission intensity in the absence and presence of quencher, respectively,  $K_q$  is a linear Stern-Volmer quenching constant and  $[Q]$  is the quencher concentration [31]. In the plots of  $F_0/F$  versus  $[Q]$ ,  $K_q$  is the slope. The quenching plots illustrate that the quenching of EB-DNA

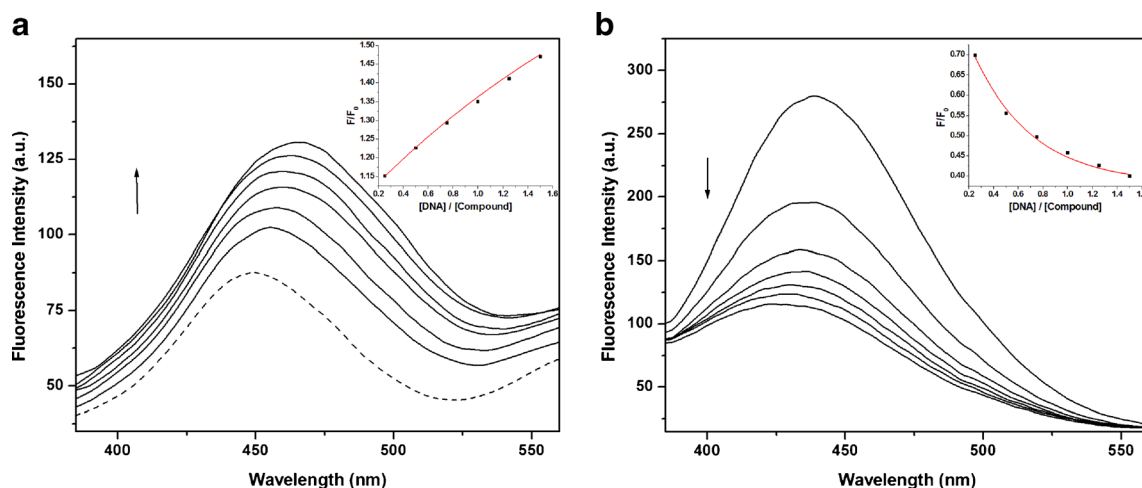


**Fig. 3** Fluorescence emission spectra of **1** (a) and **2** (b) upon addition of ct DNA. ( $\lambda_{\text{ex}}=320 \text{ nm}$ ,  $\lambda_{\text{em}}=350\text{--}600 \text{ nm}$ )  $C_{\text{xanthenes}}=10 \mu\text{M}$ ,  $C_{\text{DNA}}=0, 2.5, 5, 7.5, 10, 12.5, 15 \mu\text{M}$ . The arrow indicates the fluorescence

changes upon increasing DNA concentration. The inset is plot of  $F/F_0$  versus  $[\text{DNA}]/[\text{compound}]$

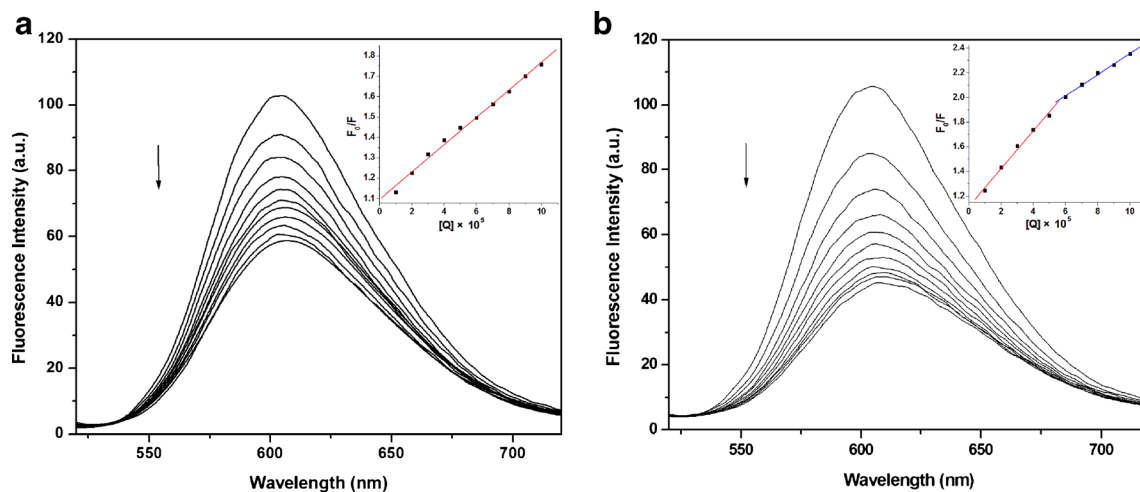


**Fig. 4** Fluorescence emission spectra of DNA-EB in the absence and presence of increasing amounts of **1** (a) and **2** (b). ( $\lambda_{\text{ex}}=500$  nm,  $\lambda_{\text{em}}=520\text{--}720$  nm)  $C_{\text{EB}}=2$   $\mu\text{M}$ ,  $C_{\text{DNA}}=30$   $\mu\text{M}$ ,  $C_{\text{xanthones}}=0, 2.5, 5, 7.5, 10$ ,

12.5, 15, 17.5, 20, 22.5, 25  $\mu\text{M}$ . The arrow indicates the fluorescence decreases upon increasing DNA concentration. The inset is Stern-Volmer quenching plots

adduct by **1** is in good agreement with the linear Stern-Volmer equation (Fig. 8a, inset). And the  $K_q$  value for **1** is  $0.67 \times 10^4 \text{ M}^{-1}$ , which shows only one quenching process, indicating that **1** intercalates into DNA. However, there are two quenching processes in the DNA-EB adduct competitive binding with **2** (Fig. 8b, inset), the  $K_q$  value is  $1.53 \times 10^4 \text{ M}^{-1}$  and  $0.85 \times 10^4 \text{ M}^{-1}$ , respectively. These indicate **2** can intercalate into the DNA base pairs by the xanthone plane and bind the DNA phosphate groups by the basic amine alkyl chain. The results are consistent with the above spectroscopic analysis.

#### Circular Dichroic Spectra

CD spectra techniques give us useful information on how the DNA conformation is influenced by the binding of small molecules. The CD spectrum of free ct DNA consists of a positive band at 277 nm due to base stacking and a negative band at 246 nm due to the polynucleotide helicity, which is characteristic of DNA in the right-handed B form [32]. The changes in CD signals of DNA are observed on interaction with small molecules may often be assigned to the corresponding changes in DNA structure. Thus simple groove binding and electrostatic interaction of small molecules shows less or no perturbation on the base-stacking and helicity bands, whereas intercalation enhances the intensities of both the bands stabilizing the right-handed B conformation of DNA as observed for the classical intercalator [33].

The CD spectra of DNA are monitored in the presence of xanthones. The changes are shown in Fig. 5. The large increase in the DNA stacking band reveals the effect of strong intercalation of the xanthones on base stacking. It is possible that the extended aromatic rings reduce the helical twist angle of the DNA base pairs and increase the intensity of the base

stacking band [34]. The large decrease in the DNA helicity band indicates that DNA is unwound upon interaction with the compounds and then transformed into other conformations. Furthermore, **2** shows more evident influence than **1** on the conformation of DNA.

#### Agarose Gel Electrophoresis Assay

The binding modes of xanthones to pUC18 plasmid DNA are further examined by agarose gel electrophoresis assay. As shown in Fig. 6, the migration rate of DNA decreases obviously in the Form I (supercoiled form) and the Form II (relaxed form) with increasing concentrations of **1–2** from 25 to 50  $\mu\text{M}$ . This phenomenon is similar to that of EB [35]. The migration rate of DNA shows a more obvious decrease in

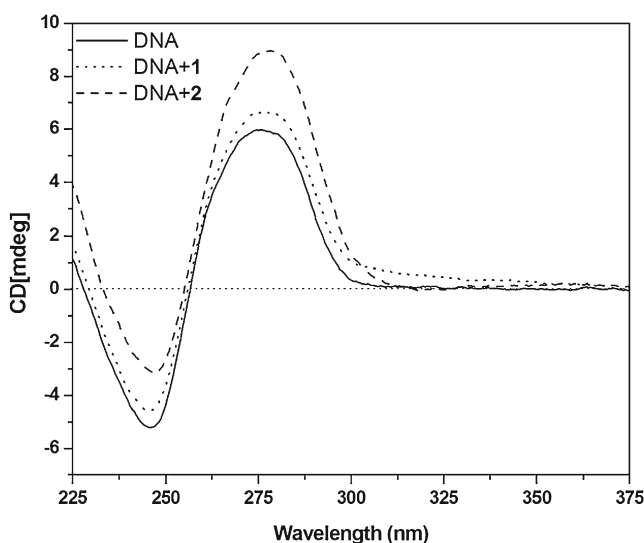


**Fig. 5** CD spectra of ct DNA (60  $\mu\text{M}$ ) in the absence and presence of xanthones **1–2** (20  $\mu\text{M}$ )

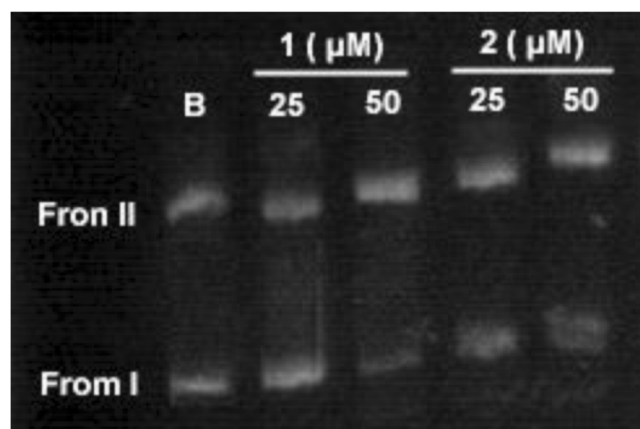


**Fig. 6** The electrophoretic migration assays of pUC18 DNA incubated with xanthenes 1–2. B represents blank; the concentration of 1–2 is indicated in the figure

the case of **2**. This once again confirms a stronger intercalative effect of **2** to DNA than **1**. This result is very intuitive and agrees with the above spectra results.

#### PCR Amplification

To study the influence of xanthenes on DNA amplification, the sequences of primer pairs are designated as 5'TCAGGTTCAGGGGAGGTGTG3' (forward) and 5'AAGGCTACGTCCAGGAGCGCA3' (reverse) in order to amplify the defined fragment between site 950 and 1,491 of plasmid pEGFP-N1 via PCR. The results are shown in Fig. 7. A band of 542 bp is seen on agarose gel while xanthenes is absent within PCR system (lane b in Fig. 7). In the control group, addition of xanthenes (5  $\mu$ M) does not prevented PCR, indicates that they have no effect on Taq DNA polymerase (lane c, f in Fig. 7). In the experimental group, the PCR product is barely visible on agarose gel while forward primer or reverse primer pre-incubated for 6 h at 4  $^{\circ}$ C with **2** (5  $\mu$ M) (lane g, h in Fig. 7). The similar result does not appear in the case of **1** (lane d, e, in Fig. 7). Therefore, it is concluded from these data that **2** is able to bind single stranded DNA, thereby preventing DNA amplification. This is a great proof of the spectroscopy inference.

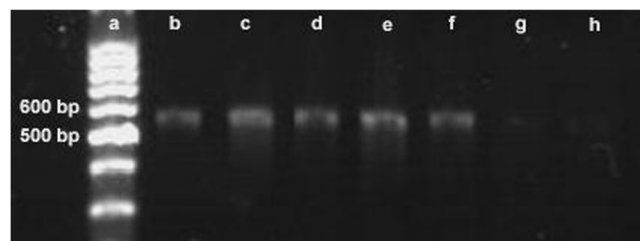


**Fig. 7** The effect of xanthenes on PCR. a: DNA ladder; b: PCR without xanthenes; c, f: PCR with **1** (5  $\mu$ M) and **2** (5  $\mu$ M), respectively; d, e: **1** (5  $\mu$ M) pre-incubated for 6 h at 4  $^{\circ}$ C with forward primer and reverse primer, respectively; g, h: **2** (5  $\mu$ M) pre-incubated for 6 h at 4  $^{\circ}$ C with forward primer and reverse primer, respectively

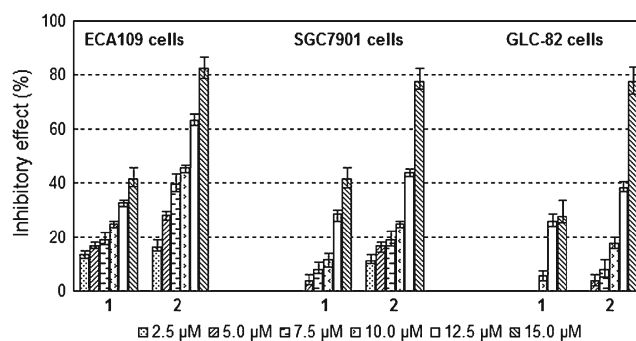


**Fig. 8** Inhibition on various human cancer cells proliferation activity of xanthenes 1–2

#### In Vitro Antitumor Potency

To evaluate the potential antitumor activity of xanthenes, three human cancer cell lines (ECA109, SGC7901, GLC-82) are incubated for 72 h with varying concentrations of them and the cell viability is determined by the MTT assay in vitro. The inhibitory effect is increased in response to xanthenes 1–2 in a dose-dependent manner as illustrated in Fig. 8. The two compounds exhibit potent inhibition activity against three human tumor cell lines. And **2** with the polar amine group has a better hydrophilicity and penetration for cell membrane, therefore, it exhibits more significant antitumor activity (Table 1). Combining with the DNA-binding experiment, it may be because the compounds intercalate into the base group pairs of DNA, which induce damage to DNA in the cancer cells, inhibiting the division of cancer cells and resulting in cell death [36]. In addition, amine moiety with high pKa value is more likely to be protonated and develop a cationic charge, therefore, binding with the phosphate groups of DNA and blocking DNA replication.

The flexible chain with active group linked at rigid xanthone plane may tune the DNA binding mode and facilitate the DNA selective binding, which imply that the suitable substituents in xanthone derivatives might contribute to the increase of their anticancer activity or to the decrease of their toxicity. Because of the multiple structures and compositions in various tumor cell lines, the complicated mechanisms about the effect of the compounds on the tumor cells are currently under the way.

**Table 1** The IC<sub>50</sub> values of xanthenes 1–2 against various human cancer cells

| Compound | IC <sub>50</sub> ( $\mu$ M) |         |        |
|----------|-----------------------------|---------|--------|
|          | ECA109                      | SGC7901 | GLC-82 |
| <b>1</b> | 25.67                       | 33.16   | >50    |
| <b>2</b> | 9.56                        | 13.31   | 16.05  |

## Conclusion

The DNA binding properties of xanthenes have been investigated by spectroscopic methods, electrophoretic migration assay and polymerase chain reaction test. The results indicate that xanthenes can insert DNA depending on the good planarity of aromatic ring and the xanthone with amine side chain would bind the DNA phosphate groups, thereby showing a better DNA binding ability than the xanthone. Comparing the inhibitory effect in vitro, the xanthone with amine side chain exhibits more significant antitumor activity, which accord with the results of DNA binding study. And each compound would show the cytotoxic activity varying according to the various tumor cells. We conclude that the xanthenes intercalate into DNA and cause DNA damage in cancer cells, and the xanthone with amine side chain is able to bind single stranded DNA to prevent DNA amplification, thus inhibiting the proliferation of cancer cells. Information obtained from the present work provides evidence for DNA binding property of xanthenes and is expected to offer further impetus for developing novel DNA targeted therapeutic agents.

**Acknowledgement** We are grateful for the financial support of the Natural Science Foundation of Hebei Province of China (B2012201132) and the Scientific Research Foundation of Hebei University (2010–204). We are also grateful for the kind help of Professor Yali Song.

## References

- Chen SX, Zhang DY, Seelig G (2013) Conditionally fluorescent molecular probes for detecting single base changes in double-stranded DNA. *Nat Chem* 5(9):782–789
- Gill MR, Thomas JA (2012) Ruthenium(II) polypyridyl complexes and DNA-from structural probes to cellular imaging and therapeutics. *Chem Soc Rev* 41(8):3179–3192
- Keenea FR, Smitha JA, Collins JG (2009) Metal complexes as structure-selective binding agents for nucleic acids. *Coord Chem Rev* 253(15–16):2021–2035
- Muzikar KA, Meier JL, Gubler DA, Raskatov JA, Dervan PB (2011) Expanding the repertoire of natural product-inspired ring pairs for molecular recognition of DNA. *Org Lett* 13(20):5612–5615
- Chenoweth DM, Meier JL, Dervan PB (2013) Pyrrole-imidazole polyamides distinguish between double-helical DNA and RNA. *Angew Chem Int Edit* 52(1):415–418
- Morinaga H, Bando T, Takagaki T, Yamamoto M, Hashiya K, Sugiyama H (2011) Cysteine cyclic pyrrole–imidazole polyamide for sequence-specific recognition in the DNA minor groove. *J Am Chem Soc* 133(46):18924–18930
- Banerjee S, Veale EB, Phelan CM, Murphy SA, Tocci GM, Gillespie LJ, Frimannsson DO, Kelly JM, Gunnlaugsson T (2013) Recent advances in the development of 1, 8-naphthalimide based DNA targeting binders, anticancer and fluorescent cellular imaging agents. *Chem Soc Rev* 42(3):1601–1618
- Chichirovsky M, Eloy L, Jullien H, Saker L, Ségal-Bendirdjian E, Poupon J, Bombard S, Cresteil T, Retailleau P, Marinetti A (2013) Antitumor trans-N-heterocyclic carbene–amine–Pt (II) complexes: synthesis of dinuclear species and exploratory investigations of DNA binding and cytotoxicity mechanisms. *J Med Chem* 56(5):2074–2086
- Kalaivani P, Prabhakaran R, Poomima P, Dallemer F, Vijayalakshmi K, Vijaya Padma V, Natarajan K (2012) Versatile coordination behavior of salicylaldehydethiosemicarbazone in Ruthenium (II) carbonyl complexes: synthesis, spectral, X-ray, electrochemistry, DNA binding, cytotoxicity, and cellular uptake studies. *Organometallics* 31(23):8323–8332
- Busto N, Valladolid J, Martínez-Alonso M, Lozano HJ, Jalón FA, Manzano BR, Rodríguez AM, Carrión MC, Biver T, Leal JM, Espino G, García B (2013) Anticancer activity and DNA binding of a bifunctional Ru (II) arene aqua-complex with the 2, 4-diamino-6-(2-pyridyl)-1, 3, 5-triazine ligand. *Inorg Chem* 52(17):9962–9974
- Martínez R, Chacón-García L (2005) The search of DNA-intercalators as antitumoral drugs: what it worked and what did not work. *Curr Med Chem* 12(2):127–151
- Zwang TJ, Singh K, Johal MS, Selassie CR (2013) Elucidation of the molecular interaction between cisplatin and flavonol (s) and their effect on DNA binding. *J Med Chem* 56(4):1491–1498
- Jarak I, Marjanovi M, Piantanida I, Kralj M, Karminski-Zamola G (2011) Novel pentamidine derivatives: synthesis, anti-tumor properties and polynucleotide-binding activities. *Eur J Med Chem* 46(7):2807–2815
- Engelhard DM, Pievo R, Clever GH (2013) Reversible stabilization of transition-metal-binding DNA G-quadruplexes. *Angew Chem Int Edit* 52(49):12843–12847
- Ramakrishnan S, Suresh E, Riyasdeen A, Akbarsha MA, Palaniandavar M (2011) Interaction of rac-[M(diimine)<sub>3</sub>]<sup>2+</sup> (M = Co, Ni) complexes with ct DNA: role of 5,6-dmp ligand on DNA binding and cleavage and cytotoxicity. *Dalton Trans* 40:3245–3256
- Pouli N, Marakos P (2009) Fused xanthone derivatives as antiproliferative agents. *Anticancer Agents Med Chem* 9(1):77–98
- Park SE, Chang IH, Jun KY, Lee E, Lee ES, Na Y, Kwon Y (2013) 3-(3-Butylamino-2-hydroxy-propoxy)-1-hydroxy-xanthen-9-one acts as a topoisomerase II $\alpha$  catalytic inhibitor with low DNA damage. *Eur J Med Chem* 69(11):139–145
- Zou HX, Koh JJ, Li JG, Qiu SX, Aung TT, Lin HF, Lakshminarayanan R, Dai XP, Tang C, Lim FH, Zhou L, Tan AL, Verm C, Tan DTH, Hardy Sze On Chan HSO, Saraswathi P, Cao D, Liu SP, Beuerman RW (2013) Design and synthesis of amphiphilic xanthone-based, membrane-targeting antimicrobials with improved membrane selectivity. *J Med Chem* 56(6):2359–2373
- Wang HF, Shen R, Tang N (2009) Synthesis and characterization of the Zn (II) and Cu (II) piperidinyli soeoxanthone complexes: DNA-binding and cytotoxic activity. *Eur J Med Chem* 44(11):4509–4515
- Shen R, Wang P, Tang N (2010) Cytotoxic activity and DNA-binding properties of xanthone derivatives. *J Fluoresc* 20(6):1287–1297
- Liu Y, Zou L, Ma L, Chen WH, Wang B, Xu ZL (2006) Synthesis and pharmacological activities of xanthone derivatives as  $\alpha$ -glucosidase inhibitors. *Bioorg Med Chem* 14(16):5683–5690
- Kumar CV, Asuncion EH (1993) DNA binding studies and site selective fluorescence sensitization of an anthryl probe. *J Am Chem Soc* 115(19):8547–8553
- Huang CZ, Li YF, Feng P (2001) A spectrophotometric study on the interaction of neutral red with double-stranded DNA in large excess. *Talanta* 55(2):321–328
- Bloomfield VA, Crothers DM, Tinoco I Jr (1974) Physical chemistry of nucleic acids. Harper & Row, New York, pp 429–476
- Kelly JM, Murphy MJ, McConnell DJ, OhUigin C (1985) A comparative study of the interaction of 5,10,15,20-tetrakis (N-methylpyridinium-4-yl)porphyrin and its zinc complex with DNA using fluorescence spectroscopy and topoisomerisation. *Nucleic Acids Res* 13:167–184

26. Wolf A, Shimer GH Jr, Meehan T (1987) Polycyclic aromatic hydrocarbons physically intercalate into duplex regions of denatured DNA. *Biochemistry* 26(20):6392–6396
27. Satyanarayana S, Dabrowiak JC, Chaires JB (1992) Neither  $\Delta$ - nor  $\Lambda$ -tris(phenanthroline) ruthenium(II) binds to DNA by classical intercalation. *Biochemistry* 31(39):9319–9324
28. Lippard SJ (1978) Platinum complexes: probes of polynucleotide structure and antitumor drugs. *Acc Chem Res* 11(5):211–217
29. Zeng YB, Yang N, Liu WS, Tang N (2003) Synthesis, characterization and DNA-binding properties of La (III) complex of chrysin. *J Inorg Biochem* 97(3):258–264
30. Kumar CV, Barton JK, Turro NJ (1985) Photophysics of ruthenium complexes bound to double helical DNA. *J Am Chem Soc* 107(19):5518–5523
31. Eftink MR, Ghiron CA (1981) Fluorescence quenching studies with proteins. *Anal Biochem* 114(2):199–227
32. Ivanov VI, Minchenkova LE, Schyolkina AK, Poletayev AI (1973) Different conformations of double-stranded nucleic acid in solution as revealed by circular dichroism. *Biopolymers* 12(1):89–110
33. Lincoln P, Tuite E, Nordén B (1997) Short-circuiting the molecular wire: cooperative binding of  $\Delta$ -[Ru(phen)<sub>2</sub>dppz]<sup>2+</sup> and  $\Delta$ -[Rh(phi)2bipy]<sup>3+</sup> to DNA. *J Am Chem Soc* 119(6):1454–1455
34. Nordén B, Tjerneld F (1982) Structure of methylene blue-DNA complexes studied by linear and circular dichroism spectroscopy. *Biopolymers* 21(9):1713–1734
35. Baraldi PG, Bovero A, Fruttarolo F, Preti D, Tabrizi MA, Pavani MG, Romagnoli R (2004) DNA minor groove binders as potential antitumor and antimicrobial agents. *Med Res Rev* 24(4):475–528
36. Zuber G, Quada JC Jr, Hecht SM (1998) Sequence selective cleavage of a DNA octanucleotide by chlorinated bithiazoles and bleomycins. *J Am Chem Soc* 120(36):9368–9369